IFIC/97-29
FTUV/97-30
July 24, 2013

Charmonia Production in Hadron Colliders and the Extraction of Colour-Octet Matrix Elements *

B. Cano-Coloma and M.A. Sanchis-Lozano †‡

Instituto de Física Corpuscular (IFIC), Centro Mixto Universidad de Valencia-CSIC
and
Departamento de Física Teórica
Dr. Moliner 50, E-46100 Burjassot, Valencia (Spain)

July 24, 2013

Abstract

We present the results of our analysis on charmonia (J/ψ and ψ') hadroproduction taking into account higher-order QCD effects induced by initial-state radiation in a Monte Carlo framework, with the colour-octet mechanism implemented in the event generation. We find that those colour-octet matrix elements extracted so far from Fermilab Tevatron data for both J/ψ and ψ' production have to be lowered significantly. We finally make predictions for charmonia production at the LHC, presenting a simple code for a *fast* simulation with PYTHIA based on the colour-octet model.

PACS: 12.38.Aw; 13.85.Ni
Keywords: Quarkonia production; Color-Octet; NRQCD; LHC; Tevatron

*Research partially supported by CICYT under grant AEN-96/1718
†Corresponding author
‡E-mail:mas@evalvx.ific.uv.es ; Phone: +34 6 386 4752 ; Fax : +34 6 386 4583

1 Introduction

Likely, the Large Hadron Collider or LHC will become operative by the beginning of the next century, offering a wide programme of exciting possibilities in Particle Physics, among which the origin of mass at the electroweak scale and the possible discovery of supersymmetric particles, the investigation of CP violation in B mesons and detailed studies of top quark physics. Other interesting topics related to charm and beauty flavours will be covered as well benefitting of a foreseen huge statistics to be collected with the machine running even at "low" luminosity ($\simeq 10^{33}$ cm$^2 s^{-1}$) [1] [2]. Following this line of research, we shall focus in this paper on inclusive hadroproduction of heavy resonances, in particular charmonia J/ψ and ψ' states, whose relevance in the study of perturbative and non-perturbative QCD will be briefly reviewed.

To first approximation, heavy-flavour hadroproduction can be treated in the framework of perturbative QCD due to the relatively large quark masses [3] and consequently the partonic production cross sections can be convoluted with parton distribution functions (PDF's) of the colliding protons. This scheme can indeed be viewed as well founded since the underlying parton interaction is hard, therefore providing a reasonable justification for such a factorization of the production process. Higher-order corrections to the matrix elements of the short-distance processes may be incorporated likely improving the accuracy of the predicted cross sections. Even complex effects such as multiple gluon emission can be treated analytically according to resummation techniques [4].

Nevertheless, such an essentially analytic approach may eventually oversight the real complexity of the full hadronic collision and a certain amount of modifications should be added if a more realistic description is required. For example, parton evolution either at the initial or final state together with fragmentation and recombination of the beam remnants could play an important rôle leading to substantial modifications in the final state, even for inclusive processes.

On the other hand, event generators based on a Monte Carlo framework represent an alternative philosophy of coping with the complexity of very high energy hadronic reactions by dividing the full problem in a set of components to be dealt separately in a simulation chain. The hard partonic interaction, constituting the underlying or skeleton process of the simulation, is dressed up with soft processes leading to hundreds of final particles. Certainly, such an approach is plagued with various sources of uncertainty, especially related to the long-distance aspects of the strong interaction dynamics, associated to the assumptions and modelling of the generation. However, the impressive amount of collected experimental data used in a heuristic way to *tune* those parameters of the event generator, gives reliability to this method to a considerable degree providing a powerful tool to interpret current data and make sensible predictions for future experiments.

In this work we re-examine prompt production of heavy resonances at high-energy hadron colliders by means of the event generator PYTHIA [5]. Undoubtedly, there is a widespread recognition that the study of heavy quarkonia has been playing an important

rôle over the past decades in the development of the theory of the strong interaction and such beneficial influence seems far from ending. Moreover, a precise understanding of prompt charmonia production offer several advantages from both experimental and theoretical points of view at the LHC.

The fact that both J/ψ and ψ' resonances can decay into a oppositely charged lepton pair with a respectable branching fraction (especially the former), permits its discrimination in a huge hadronic background. Actually, charmonia production can be viewed as interesting in its own right for precise tests of both perturbative and non-perturbative QCD, search for exotic states or as a probe of the parton content of the proton. Furthermore, completely different processes as for example the decay $B_d^0 \to J/\psi K_s^0$, a golden channel to investigate CP violation in B decays, require a precise estimate of sources of background coming from random combinations involving prompt J/ψ's.

On the other hand, the experimental discovery at Fermilab [6] of an excess of inclusive production of prompt heavy quarkonia (mainly for J/ψ and ψ' resonances) in antiproton-proton collisions triggered an intense theoretical activity beyond what was considered conventional wisdom until recently [7] [8]. The discrepancy between the so-called colour-singlet model (CSM) in hadroproduction [9, 10] and the experimental data amounts to more than an order of magnitude and cannot be attributed to those theoretical uncertainties arising from the ambiguities on the choice of a particular parton distribution function, the heavy quark mass or different energy scales.

The colour-singlet model assumes that the heavy quark pair is produced in a colour-singlet state with the right quantum numbers already during the hard collision. The production cross section involves a perturbative calculation where the proper spin and angular momentum states are projected out, and the non-perturbative component of the hadronization comes from a single parameter to be identified with the wave function of the resonance at the origin (or its derivatives for non S-wave states). The fact that the latter can be derived from potential models fitting the charmonia spectrum or from their leptonic decay modes, gives its predictive power to the colour-singlet model. However, as mentioned above, such predictions stand quite below the experimental yield at high-p_t, so that some modifications have to be done. In addition, it should be emphasized that the model is clearly incomplete since relativistic corrections due to the relative velocity of quarks in the bound state are ignored - expected to be sizeable especially for charmonia. Moreover, another hint of the incompleteness of the CSM comes from the existence of infrared divergences in the production cross section for P-wave states, which cannot be absorbed in its non-perturbative factor.

In order to resolve all these difficulties, it has been recently argued that the heavy quark pair not necessarily has to be produced in a colour-singlet state at the short-distance partonic process itself [11]. Alternatively, it can be produced in a colour-octet state evolving non-perturbatively into quarkonium in a specific final state with the correct quantum numbers according to some computable probabilities governed by the internal velocity of the heavy quark. This mechanism, usually named as the colour-octet

model (COM) [1], can be cast into the rigorous framework of an effective non-relativistic theory for the strong interactions (NRQCD) deriving from first principles [13].

However, the weakness of the COM lies in the fact that the non-perturbative parameters characterizing the long-distance hadronization process beyond the colour-singlet contribution (i.e. the colour-octet matrix elements) are so far almost free parameters to be adjusted from the fit to experimental data, though expected to be mutually consistent according to the NRQCD power scaling rules, or to resort to non-perturbative models [14].

On the other hand, an attractive feature of the colour-octet hypothesis consists of the universality of the NRQCD matrix elements (ME) entering in other charmonium production processes like photoproduction [15]. Let us look below in some detail at the way hadronization is folded with the partonic description of hadrons, focusing for concreteness on the couple of related papers [16, 17].

In the first paper [16], Cho and Leibovich considered for charmonium production (in addition to the CSM) the ${}^3S_1$ coloured intermediate state as a first approach, computing the matrix elements as products of perturbative parts for the short-distance partonic processes, and the colour-octet ME concerning the long-distance hadronization. Finally, a convolution of concrete parton distribution functions and the differential cross-section for the $Q\bar{Q}$ production subprocess was performed, whereby the p_t dependence of the charmonia production exclusively coming from the latter.

In Ref. [17] the same authors take into account further contributions from new coloured states (for more details see the quoted references) concluding finally that at high enough p_t a two-parameter fit is actually required to explain the observed inclusive p_t distribution of charmonia production at the Fermilab Tevatron.

Notice, however, that such calculations were carried out based on a possibly oversimplified picture of the hadronic interaction. Indeed, it is well-known for a long time that higher-order effects (K factors) play an important rôle in inclusive hadroproduction. In particular, beyond the primordial transverse momentum k_t of partons in hadrons related to Fermi motion relevant at small p_t, initial-state radiation of gluons by the interacting partons add up to yield an *effective* intrinsic transverse momentum which certainly has to be considered in hadroproduction at high p_t [18]. As we shall see, if overlooked at all, the effect on the fit parameters (and ultimately on the colour-octet ME's) amounts to a *systematic* overestimate.

In fact, one should distinguish the primordial transverse momentum of partons owing to their Fermi motion (a non-perturbative effect) from the perturbative contribution dynamically generated via gluon radiation generally implemented in the event generators by means of a parton shower algorithm [19] [2]. By *effective* k_t we merge both effects

[1] For the sake of brevity in our theoretical introduction we do not expose another approach to heavy quarkonia production in the same spirit as the COM but based on duality arguments known as the colour-evaporation model, referring the reader to [12] and references therein

[2] However, it is not yet completely clear how to separate uniquely both components from real experimental data [18]

under a common name, though the former is actually overshadowed by the latter at high p_t. Of course, the PYTHIA treatment of the effective k_t is not guaranteed to be perfect but, nevertheless, should give a reasonable estimate of such effects.

In this work we have extended our earlier analysis of J/ψ hadroproduction at colliders [20] [21] to the ψ' state, affording a more complete test upon the validity of the NRQCD power scaling rules relating different long-distance matrix elements. The paper is organized as follows. In Section 2 we describe the hard processes considered for charmonia hadroproduction and we discuss their implementation in the event generator PYTHIA, described in more detail in the Appendix at the end of the paper where we also present a code for a fast simulation of charmonia using PYTHIA. In Section 3 we perform new fits to Tevatron data on prompt J/ψ and ψ' direct production extracting NRQCD matrix elements from them. We finally make some predictions for charmonia direct production at the LHC in Section 4.

2 Implementation of the COM in PYTHIA

Originally, the event generator PYTHIA [5] produces direct J/ψ's and higher χ_{cJ} resonances in hadron-hadron collisions according to the CSM. However, as already mentioned this model fails off to account for the charmonia production rate at the Fermilab Tevatron by more than an order of magnitude. Consequently, we have implemented a code in PYTHIA in order to include the colour-octet mechanism for J/ψ hadroproduction (ψ' generation has been based upon the same set of production channels) via the following α_s^3 partonic processes:

- $g \ + \ g \rightarrow J/\psi \ + \ g$
- $g \ + \ q \rightarrow J/\psi \ + \ q$
- $q \ + \ \bar{q} \rightarrow J/\psi \ + \ g$

We have included in the simulation the ${}^3S_1^{(8)}$, ${}^1S_0^{(8)}$ and ${}^3P_J^{(8)}$ $(J = 0, 1, 2)$ states in ${}^3S_1$ charmonia hadroproduction according to the COM [17]. The squared amplitudes, taken from Refs. [16, 17] are reproduced below. Firstly let us consider the ${}^3S_1^{(8)}$ intermediate state:

$$\begin{aligned}\overline{\sum}|\mathcal{A}(gg\rightarrow J/\psi g)|^2 &= -\frac{8\pi^3\alpha_s^3}{9M^3}\,\frac{27(\hat{s}\hat{t}+\hat{t}\hat{u}+\hat{u}\hat{s})-19M^4}{[(\hat{s}-M^2)(\hat{t}-M^2)(\hat{u}-M^2)]^2} \\ &\times \ [(\hat{t}^2+\hat{t}\hat{u}+\hat{u}^2)^2 - M^2(\hat{t}+\hat{u})(2\hat{t}^2+\hat{t}\hat{u}+2\hat{u}^2) + M^4(\hat{t}^2+\hat{t}\hat{u}+\hat{u}^2)] \\ &\times \ <0|O_8^{J/\psi}({}^3S_1)|0> \qquad (1)\end{aligned}$$

$$\overline{\sum}|\mathcal{A}(gq\rightarrow J/\psi q)|^2 = -\frac{16\pi^3\alpha_s^3}{27M^3}\,\frac{\hat{s}^2+\hat{u}^2+2M^2\hat{t}}{\hat{s}\hat{u}(\hat{t}-M^2)^2}[4(\hat{s}^2+\hat{u}^2)-\hat{t}\hat{u}] \ <0|O_8^{J/\psi}({}^3S_1)|0> \qquad (2)$$

$$\overline{\sum}|\mathcal{A}(q\overline{q}\rightarrow J/\psi g)|^2 \;=\; \frac{128\pi^3\alpha_s^3}{81M^3}\;\frac{\hat{t}^2+\hat{u}^2+2M^2\hat{s}}{\hat{t}\hat{u}(\hat{s}-M^2)^2}[4(\hat{t}^2+\hat{u}^2)-\hat{t}\hat{u}]\;<0|O_8^{J/\psi}(^3S_1)|0> \tag{3}$$

where the barred summation symbol refers to average over initial and final spins and colours; $\hat{s}$, $\hat{t}$ and $\hat{u}$ stand for the Mandelstam variables of the short-distance subprocesses. We shall set $M = 2M_c$ for both J/ψ and ψ' resonances in accordance with the assumption on the non-relativistic nature of heavy quarkonium made in the theoretical calculation of these amplitudes [16, 17], i.e. vanishing relative momentum of the quarks in the bound state.

The corresponding expressions for the $^1S_0^{(8)}$ contributions are:

$$\begin{aligned}\overline{\sum}|\mathcal{A}(gg\rightarrow J/\psi g)|^2 &= \frac{20\pi^3\alpha_s^3}{M}\;\frac{(\hat{s}^2-M^2\hat{s}+M^4)^2-\hat{t}\hat{u}(2\hat{t}^2+3\hat{t}\hat{u}+2\hat{u}^2)}{\hat{s}\hat{t}\hat{u}[(\hat{s}-M^2)(\hat{t}-M^2)(\hat{u}-M^2)]^2}\\ &\times\;[\hat{s}^2(\hat{s}-M^2)^2+\hat{s}\hat{t}\hat{u}(M^2-2\hat{s})+(\hat{t}\hat{u})^2]\;<0|O_8^{J/\psi}(^1S_0)|0>\end{aligned} \tag{4}$$

$$\overline{\sum}|\mathcal{A}(gq\rightarrow J/\psi q)|^2 \;=\; -\frac{40\pi^3\alpha_s^3}{9M}\;\frac{\hat{s}^2+\hat{u}^2}{\hat{t}(\hat{t}-M^2)^2}\;<0|O_8^{J/\psi}(^1S_0)|0> \tag{5}$$

$$\overline{\sum}|\mathcal{A}(q\overline{q}\rightarrow J/\psi q)|^2 \;=\; \frac{320\pi^3\alpha_s^3}{27M}\;\frac{\hat{t}^2+\hat{u}^2}{\hat{s}(\hat{s}-M^2)^2}\;<0|O_8^{J/\psi}(^1S_0)|0> \tag{6}$$

With regard to the $^3P_J^{(8)}$ contributions, they display altogether a similar (i.e. degenerate) transverse momentum behaviour as the $^1S_0^{(8)}$ component for $p_t \geq 5$ GeV [17]. Thus from a pragmatic point of view, the generation of charmonia via intermediate P-wave coloured states becomes superfluous although they must properly be taken into account in the computation of the overall cross section as explained in more detail in the Appendix.

We find from our simulation that gluon-gluon scattering actually stands for the dominant process as expected, the gluon-quark scattering contributes appreciably $\simeq 20\%$, whereas the quark-antiquark scattering represents a tiny contribution. Therefore we shall omit hereafter any further reference to the $q\overline{q}$ production channel.

Using the same numerical values for the colour-octet matrix elements as reported in Tables I and II of Ref. [17], if initial- and final-state radiation are turned off, there is a good agreement between the theoretical curve and the experimental points for both J/ψ and ψ' (see Fig. 1), as should reasonably be expected . However, if initial- and final-state radiation [3] are switched on, the predicted curve stands well above the experimental data, in accordance with the expected k_t-kick caused by the *effective*

[3] It should be noted that initial-state radiation and final-state radiation have opposite effects in the p_t spectrum, the former enhancing the high p_t tail whereas the latter softens the distribution. Indeed, in considering the process $gg\rightarrow J/\psi g$ in PYTHIA only the gluon evolves in the final state, though the energy (and momentum) of charmonium is modified as a consequence of the final-state machinery [5]

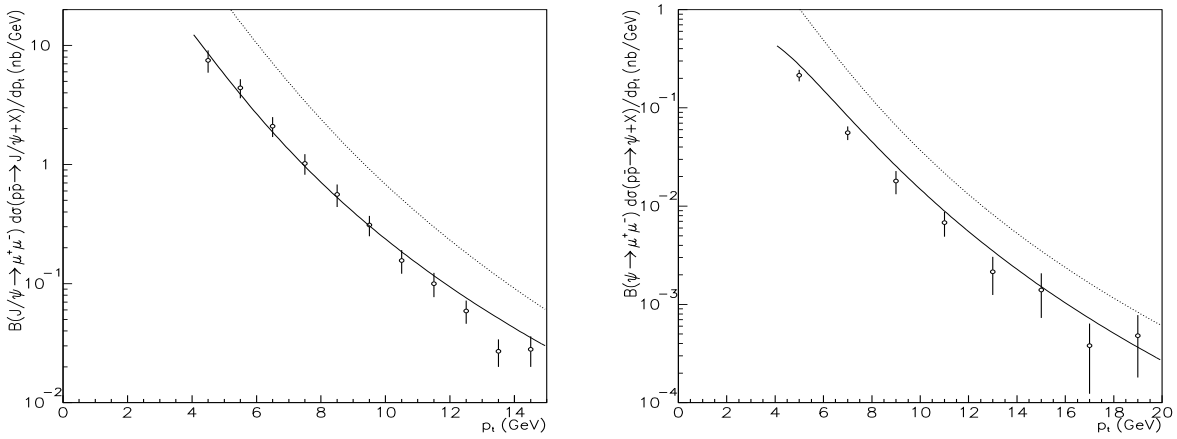

Figure 1: Curves obtained from PYTHIA (not fit) including the colour-octet mechanism for prompt J/ψ *(left)* and ψ' *(right)* production at the Tevatron using the same parameters as in Ref. [17]. The solid line corresponds to initial- and final-state radiation off and the dotted line to initial- and final-state radiation on. The MRSD0 parton distribution function and $M_c = 1.48$ GeV were employed as in [17]. All curves are multiplied by the corresponding muon branching fraction of charmonium.

intrinsic transverse momentum of partons [18]. Accordingly, keeping radiation effects in the theoretical analysis it turns out that the values for the colour-octet ME's have to be lowered by significant factors.

For the sake of clarity it is important to point out that the inclusion in the event generation of multi-gluon emission by itself almost does not change the overall cross-section for charmonia production obtained from PYTHIA. (There is however an indirect bias effect slightly increasing the cross section $\sigma(|\eta_{J/\psi}| < 0.6)$ with radiation on relative to radiation off because of the kinematical cut on the charmonia pseudorapidity.) The main effect remains in the smearing of the transverse momentum distribution leading to the enhancement of the high-p_t tail.

3 Extraction of NRQCD matrix elements from Tevatron data

In order to assess the importance of the effective intrinsic transverse momentum of partons we have made three different choices for the proton PDF [4]:

a) the leading order CTEQ 2L (by default in PYTHIA 5.7)

b) the next to leading order MRSD0 (the same as used in [17])

c) the next to leading order GRV 94 HO

[4] See [22] for technical details about the package of Parton Density Functions available at the CERN Program Library. References therein

As mentioned before, the theoretical curves for the inclusive p_t distribution of prompt J/ψ and ψ' stand in all cases above Tevatron experimental points if the set of parameters from [17] are blindly employed in the PYTHIA generation with initial-state radiation on. Motivated by this systematic discrepancy, we have performed new fits for prompt J/ψ and ψ' direct production at the Tevatron (feed-down to J/ψ from radiative decay of χ_{cJ} resonances was experimentally removed).

Those colour-octet matrix elements extracted from our analysis on J/ψ production are reported in Table 1. In Fig. 2a we plot the resulting fit to Tevatron data for the CTEQ PDF, showing separately the three different components taken into account in this work. As a figure of merit for the overall fit we found $\chi^2/N_{DF} = 1.8$. In the case of ψ' production, the respective ME's are reported in Table 2 and the corresponding plot for the CTEQ PDF is shown in figure 2b, with $\chi^2/N_{DF} = 0.4$.

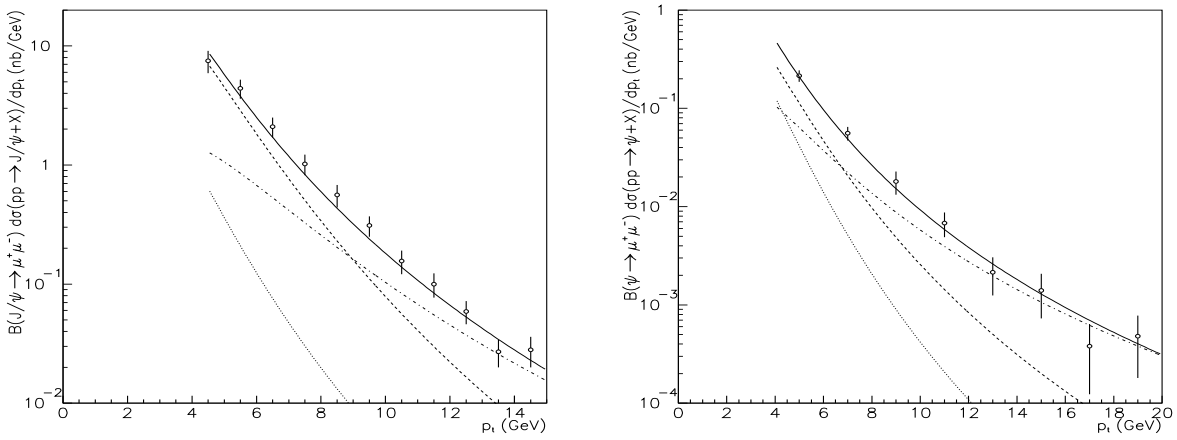

Figure 2: Two-parameter fits to the experimental Tevatron data using CSM + COM, where initial- and final-state radiation were incorporated via PYTHIA generation. a) (*left*) J/ψ and b) (*right*) ψ' production. The different contributions are shown separately i) dotted line: CSM, ii) dashed line: ${}^1S_0^{(8)}+{}^3P_J^{(8)}$, iii) dot-dashed line: ${}^3S_1^{(8)}$, iv) solid line: all contributions.

Table 1: Colour-octet matrix elements (in units of GeV^3) from the best χ^2 fit to Tevatron data on prompt J/ψ production for different parton distribution functions. The error bars are statistical only. For comparison we quote the values given in Ref. [17]: $(6.6\pm2.1)\times10^{-3}$ and $(2.2\pm0.5)\times10^{-2}$ respectively.

matrix element:	$< 0\|O_8^{J/\psi}({}^3S_1)\|0 >$	$\frac{<0\|O_8^{J/\psi}({}^3P_0)\|0>}{M_c^2} + \frac{<0\|O_8^{J/\psi}({}^1S_0)\|0>}{3}$
CTEQ2L	$(3.3\pm0.5)\times10^{-3}$	$(4.8\pm0.7)\times10^{-3}$
MRSD0	$(2.1\pm0.5)\times10^{-3}$	$(4.4\pm0.7)\times10^{-3}$
GRV 94 HO	$(3.4\pm0.4)\times10^{-3}$	$(2.0\pm0.4)\times10^{-3}$

Table 2: Colour-octet matrix elements (in units of GeV^3) from the best χ^2 fit to Tevatron data on prompt ψ' production for different parton distribution functions. The error bars are statistical only. For comparison we quote the values given in Ref. [17]: $(4.6\pm1.0)\times10^{-3}$ and $(5.9\pm1.9)\times10^{-3}$ respectively.

matrix element:	$<0\|O_8^{\psi'}(^3S_1)\|0>$	$\frac{<0\|O_8^{\psi'}(^3P_0)\|0>}{M_c^2}+\frac{<0\|O_8^{\psi'}(^1S_0)\|0>}{3}$
CTEQ2L	$(1.4\pm0.3)\times10^{-3}$	$(1.1\pm0.3)\times10^{-3}$
MRSD0	$(1.1\pm0.3)\times10^{-3}$	$(0.94\pm0.23)\times10^{-3}$
GRV 94 HO	$(1.3\pm0.2)\times10^{-3}$	$(0.12\pm0.15)\times10^{-3}$

Notice that all the ME's are lowered systematically with respect to the values reported in Ref. [17] for both J/ψ and ψ' [5]. Basically this is because initial-state radiation enhances the differential cross section for $p_t > 4$ GeV, so that the non-perturbative parameters have to be re-adjusted to restore the fit to the experimental points. Let us also remark that the combined $^1S_0^{(8)}$, $^3P_0^{(8)}$ ME's are lowered by larger factors than those for the $^3S_1^{(8)}$ contribution. Consequently, the power counting rules derived from NRQCD are more faithfully satisfied in the overall than in Ref. [17] - all of them should scale like $M_c^3 v^7$. It is especially significant that the numerical values obtained in our analysis for the $^1S_0^{(8)}+^3P_0^{(8)}$ ME's are smaller by an order of magnitude with respect to those found in Ref. [17] in accordance with the common belief widely expressed in literature [14, 23]. In this sense, theoretical expectations from the COM might be reconciled with HERA data on J/ψ photoproduction [15].

The contributions from the colour-octet $^3S_1^{(8)}$ and $^1S_0^{(8)}$ + $^3P_J^{(8)}$ states to the differential cross section for J/ψ and ψ' production are shown separately in Fig. 2. Notice that the $^1S_0^{(8)}$ and $^3P_J^{(8)}$ components dominate in both cases over the other production channels at moderate p_t, whereas the $^3S_1^{(8)}$ channel takes over at large p_t becoming asymptotically responsible of the full production rate.

Let us remark the especially relative smaller numerical values of the long-distance $^1S_0^{(8)}$, $^3P_J^{(8)}$ matrix elements regarding the GRV PDF. This is in a qualitative agreement with the fact that the MRSD0 and CTEQ2L parton distribution functions give smaller values for the gluon distribution function at small partonic x than the GRV PDF (the gluon density of the latter is steeper at small x). Hence, a gluon density with a steeper behaviour at small x steepens the p_t-spectrum for the $^3S_1^{(8)}$ component amounting to a larger production rate at moderate p_t, decreasing the $^1S_0^{(8)}+^3P_J^{(8)}$ contribution from the combined fit to the experimental inclusive distribution.

[5] A caveat is in order however. In our generation we have not included the leading log QCD corrections into the colour-octet cross section (causing the depletion of the fragmentation function of gluons into charmonium at high-p_t) through the interpolating formula (2.22) of Ref. [16]. However, final state radiation was incorporated in our analysis in contrast to Ref. [16, 17], softening the p_t inclusive distribution as mentioned in footnote #3. The neglect of those higher order QCD effects should mainly affect the high-p_t region, hence the $^3S_1$ matrix element which could be somewhat underestimated.

4 Charmonia Production at the LHC

Reliable calculations of inclusive production rates of charmonia are of considerable interest at LHC experiments in many respects [1, 2], as briefly outlined in the Intorduction. Therefore, an order-of-magnitude estimate of its production rate becomes very valuable at the present stage of the LHC experiments.

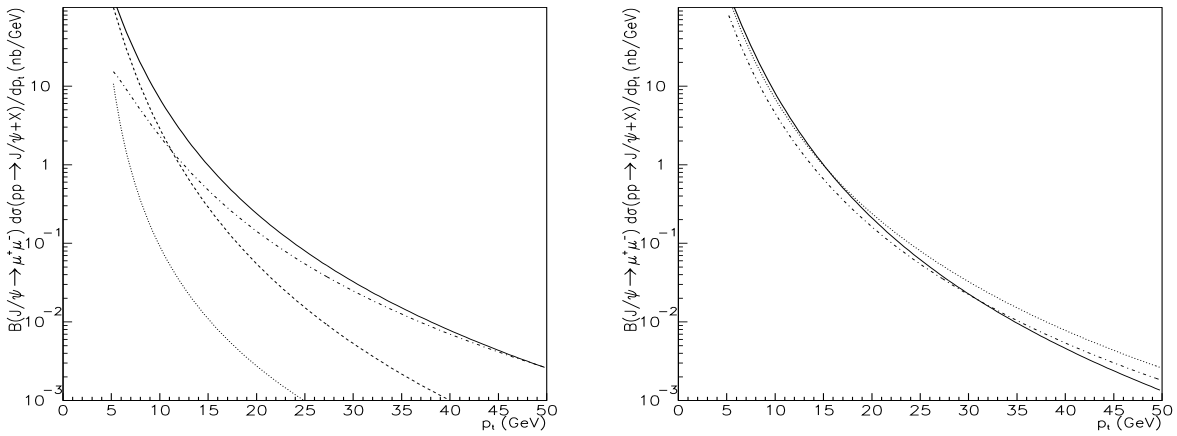

Figure 3: (*left*) Different contributions to J/ψ hadroproduction using the CTEQ PDF. The curves are labelled in the same way as in Fig. 2. ; (*right*) Our prediction for prompt J/ψ direct production at the LHC using PYTHIA with the colour-octet matrix elements from Table 1: a) dotted line: CTEQ 2L, b) dot-dashed line: MRSD0, and c) solid line: GRV HO. A rapidity cut $|y| < 2.5$ was required.

Keeping in mind such a variety of interests, we have generated direct J/ψ's and ψ's in proton-proton collisions at LHC energies (center-of-mass energy = 14 TeV) by means of our "modified" version of PYTHIA with the colour-octet ME's as shown in Tables 1 and 2 - i.e. after normalization to Tevatron data. The different contributions to J/ψ hadroproduction are depicted altogether in Fig. 3 for the CTEQ PDF.

Figure 3 also illustrates the p_t inclusive distributions of direct prompt J/ψ's at the LHC obtained for the three PDF's employed in our study. Comparing them with the distribution obtained by Sridhar [24], we find our predictions standing below his theoretical curve at large p_t. In fact this is not surprising since Sridhar considered only the ${}^3S_1^{(8)}$ coloured intermediate state, whose ME was assumed larger than the one used in this work. The argument ends by noticing that at high enough p_t the dominant production comes from the ${}^3S_1^{(8)}$ channel as the combined ${}^1S_0^{(8)} + {}^3P_J^{(8)}$ contribution falls off faster than the former.

In Fig. 4 we plot our prediction for direct ψ' production at the LHC using the CTEQ PDF, together with the J/ψ curve. From the figure it is clear that muon pair

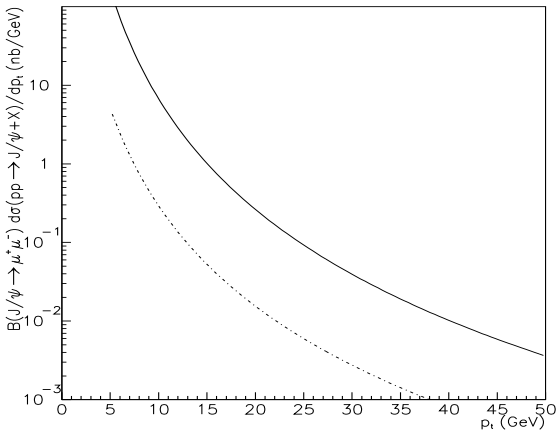

Figure 4: J/ψ (solid line) and ψ' (dash-dotted line) direct production at the LHC according to the colour-octet ME's reported in Tables 1 and 2 using the CTEQ PDF. The cut $|y| < 2.5$ was required in both cases. Both curves are multiplied by the respective branching fraction of charmonium into muons.

production from direct J/ψ is larger by more than an order of magnitude from J/ψ as compared to ψ'. It should be mentioned that our prediction for the ψ' production rate differs substancially with respect to the corresponding theoretical curve by Sridhar [24] all along the p_t range - by an order of magnitude even at moderate p_t in contrast to the J/ψ case.

5 Conclusions

In this paper we report on the extraction of long-distance colour-octet matrix elements in a Monte Carlo framework from charmonia production at hadron colliders, already studied in our previous works [20] [21], extending our analysis to the ψ' resonance. We explain in more detail the procedure followed in our investigation, also providing a code for a "fast" simulation of charmonium in hadron collisions based on the colour-octet model and compatible with the Tevatron results.

All three possible lowest order short-distance processes contributing to J/ψ hadroproduction have been taken into account, namely, $g + g \rightarrow J/\psi + g$, $g + q \rightarrow J/\psi + q$ and $q + \bar{q} \rightarrow J/\psi + g$, contributing at order α_s^3 to charmonia production including the colour-octet mechanism. The same set of channels have been considered for ψ' hadroproduction.

We have investigated higher-order effects induced by initial-state radiation, concluding that the overlooking of initial radiation leads systematically to a significant overestimate of the fit parameters. The new colour-octet matrix elements obtained for three different PDF's from Tevatron data are shown in Tables 1 and 2, which have to be

regarded as reasonable estimates due to the experimental and theoretical uncertainties. In particular, the numerical values for the combined ${}^1S_0^{(8)} + {}^3P_0^{(8)}$ matrix elements are smaller by an order of magnitude than those obtained in Ref. [17] and might resolve the difficulties of the COM found in J/ψ photoproduction at HERA [15].

Acknowledgments

We thank S. Baranov, P. Eerola, N. Ellis and M. Smizanska and the ATLAS B physics working group for useful comments and an encouraging attitude. Comments by E. Kovacs, T. Sjöstrand and K. Sridhar are also acknowledged.

Appendix

A Code for Implementing the Colour Mechanism in PYTHIA

We have modified the PYTHIA routine PYSIGH (ISUB=86) [5] for the partonic process:

$$g \ + \ g \rightarrow J/\psi \ + \ g$$

including those contributions from the ${}^3S_1^{(8)}$, ${}^1S_0^{(8)}$ and ${}^3P_J^{(8)}$ coloured states according to the expressions (1) and (4). The ME's of the latter components are related through the heavy quark spin symmetry at leading order in $1/M_c$: [13]

$$< O_8({}^3P_J) > = \ (2J+1) < O_8({}^3P_0) >$$

Moreover, it should be stressed that the colour-octet ME's associated to the ${}^1S_0^{(8)}$ and the ${}^3P_J^{(8)}$ channels cannot be disentangled from Tevatron experimental data since both are degenerate in the sense that they display a similar p_t behaviour for $p_t \geq 5$ GeV [17]. All three P-wave contributions altogether amount to about three times the ${}^1S_0$ contribution when setting $< O_8({}^3P_0) >= M_c^2 < O_8({}^1S_0) >$. Therefore one may write the following approximate equality:

$$\frac{d\sigma}{dp_t}[{}^1S_0^{(8)}] + \sum_{J=0,1,2} \frac{d\sigma}{dp_t}[{}^3P_J^{(8)}] \simeq 3 \times \frac{1}{< O_8({}^1S_0) >} \frac{d\sigma}{dp_t}[{}^1S_0^{(8)}] \times \left(\frac{< O_8({}^1S_0) >}{3} + \frac{< O_8({}^3P_0) >}{M_c^2} \right) \tag{A.1}$$

and only the ${}^1S_0^{(8)}$ component has to be simulated in practice.

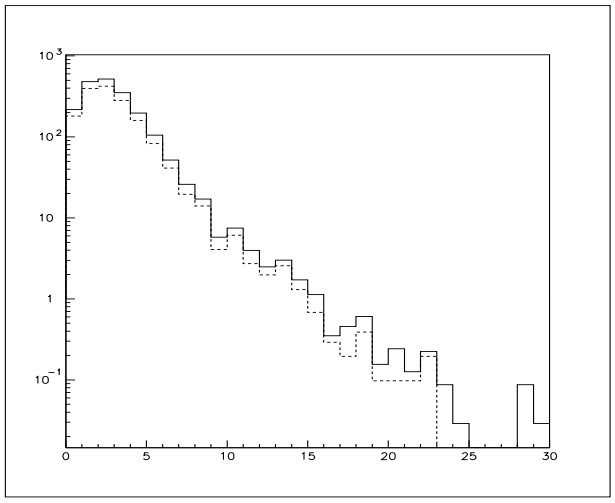

Figure 5: Histograms for $BF(J/\psi \rightarrow \mu^+\mu^-) \times d\sigma/dp_t(pp \rightarrow J/\psi X)$ obtained from PYTHIA using the CTEQ PDF at 14 TeV center-of-mass energy. Solid line: all contributions; dashed line: gg contribution.

On the other hand, we have generated with PYTHIA an event sample via the gluon-quark subprocess $g + q \rightarrow J/\psi + q$ according to the expressions (2) and (5), "adapting" for this end the PYSIGH routine ISUB=112. We found that this production channel amounts to a fraction of about 20% of the total yield of direct J/ψ's, almost constant over the p_t range under examination (see Fig. 5). Consequently, one may reduce considerably CPU time in the event generation by a slight change on the $gg \rightarrow J/\psi g$ routine, including gq scattering by means of a scaling factor. Let us note however that all the fits and plots shown in this work were performed using the gq event sample obtained from PYTHIA as explained above. The routine presented below permits a fast generation of direct J/ψ's (or ψ' with some few changes in the values of the parameters and variables such as PARP(38), SQM3, ...) in hadronic collisions at the LHC.

Thus, we have rewritten the ISUB=86 routine of PYTHIA as:

```
      ELSEIF(ISUB.EQ.86) THEN
C...g + g -> J/Psi + g.
C
C... Color-Octet Matrix Elements for J/psi
C               (CTEQ 2L)
C
         SQM3=(2.*1.48)**2
         XO83S1=0.0033
         XO81S3P=0.0048
C
C   COLOR SINGLET
C
         FACQQG1=COMFAC*AS**3*(5./9.)*PARP(38)*SQRT(SQM3)*
     &    (((SH*(SH-SQM3))**2+(TH*(TH-SQM3))**2+(UH*(UH-SQM3))**2)/
     &    ((TH-SQM3)*(UH-SQM3))**2)/(SH-SQM3)**2
C
C   COLOR OCTET (3-S-1)
C
         FACQQG2=-COMFAC*AS**3*(1./18.)*3.1416/SQRT(SQM3)*
     &    (27.*(SH*TH+TH*UH+UH*SH)-19.*SQM3**2)*((TH**2+TH*UH+UH**2)**2-
     &    SQM3*(TH+UH)*(2.*TH**2+TH*UH+2.*UH**2)+SQM3**2*
     &    (TH**2+TH*UH+UH**2))*XO83S1/
     &    ((TH-SQM3)*(UH-SQM3))**2/(SH-SQM3)**2
C
C   COLOR OCTET (1-S-0)/3 + (3-P-0) !!!
C
         FACQQG3=1000.*COMFAC*(5.*3.1416*AS**3/(4.*SQRT(SQM3)))/SH*
     &    (SH**2*(SH-SQM3)**2+SH*TH*UH*(SQM3-2.*SH)+(TH*UH)**2)/(TH*UH)*
     &    ((SH**2-SQM3*SH+SQM3**2)**2-
     &    TH*UH*(2.*TH**2+3.*TH*UH+2.*UH**2))*XO81S3P/
```

```
     &    ((TH-SQM3)*(UH-SQM3))**2/(SH-SQM3)**2
          FACQQG3=FACQQG3/1000.
C
C ... Scaling factor for g + q -> J/psi + q
C
          SCALGQ=1.25
C
          IF(KFAC(1,21)*KFAC(2,21).NE.0) THEN
             NCHN=NCHN+1
             ISIG(NCHN,1)=21
             ISIG(NCHN,2)=21
             ISIG(NCHN,3)=1
             SIGH(NCHN)=FACQQG1
             NCHN=NCHN+1
             ISIG(NCHN,1)=21
             ISIG(NCHN,2)=21
             ISIG(NCHN,3)=1
             SIGH(NCHN)=FACQQG2*SCALGQ
             NCHN=NCHN+1
             ISIG(NCHN,1)=21
             ISIG(NCHN,2)=21
             ISIG(NCHN,3)=1
             SIGH(NCHN)=3.*FACQQG3*SCALGQ
          ENDIF
```

The following variables, originally not present in PYTHIA, have been specifically introduced in our routine:

- XO83S1: colour-octet ME associated to the ${}^3S_1$ component
- XO81S3P: linear combination $< O_8({}^1S_0) > /3 + < O_8({}^3P_0) > /M_c^2$
- SCALGQ: scaling factor taking into account gq production

A lower cut-off was used throughout in the event generation ($p_{tmin} = 1$ GeV by default in PYTHIA for processes singular at $p_t \to 0$) thereby avoiding the problematic low-p_t region for charmonia hadroproduction. The effect of such a cut on the experimentally observed p_t range ($p_t > 4$ GeV) is rather small, representing a slight underestimation of the production rate in the event generation with radiation on as a consequence of the ISR effect [18].

Lastly, let us point out that the theoretical curves appearing in all our plots were obtained from histograms (filled with the corresponding PYTHIA ouput data) fitted by means of the four-parameter p_t function:

$$F[\alpha_1, \alpha_2, \alpha_3, \alpha_4; p_t] \;=\; \alpha_1 \; \frac{p_t^{\alpha_2}}{(\alpha_3 + p_t^2)^{\alpha_4}} \tag{A.2}$$

providing an excellent fit in the whole p_t range examined.

References

[1] Technical Proposal of the ATLAS Collaboration, CERN/LHCC 94-43 (1994)

[2] Technical Proposal of the CMS Collaboration, CERN/LHCC 94-38 (1994)

[3] P. Nason, S. Dawson, R.K. Ellis, Nucl. Phys. **B303** (1988) 607

[4] S. Catani, Nucl. Phys. B (Proc. Suppl.) **54A** (1997) 107

[5] T. Sjöstrand, Comp. Phys. Comm. **82** (1994) 74

[6] CDF Collaboration, F. Abe at al., Phys. Rev. Lett. **69** (1992) 3704; D0 Collaboration, V. Papadimitriou et al., Fermilab-Conf-95/128-E

[7] M. Cacciari, M. Greco, M.L. Mangano and A. Petrelli, Phys. Lett. **B356** (1995) 553

[8] M. Beneke, CENR-TH/97-55 (hep-ph/9703429)

[9] R. Baier, R. Rückl, Z. Phys. **C19** (1983) 251

[10] G.A. Schuler, CERN-TH-7170-94 (hep-ph/9403387)

[11] E. Braaten and S. Fleming, Phys. Rev. Lett. **74** (1995) 3327

[12] G.A. Schuler, Z. Phys. **C71** (1996) 317

[13] G.T. Bodwin, E. Braaten, G.P. Lepage, Phys. Rev. **D51** (1995) 1125

[14] G.A. Schuler, CERN-TH/97-12 (hep-ph/9702230)

[15] M. Cacciari and M. Krämer, Phys. Rev. Lett. **76** (1996) 4128

[16] P. Cho and A.K. Leibovich, Phys. Rev. **D53** (1996) 150

[17] P. Cho and A.K. Leibovich, Phys. Rev. **D53** (1996) 6203

[18] L. Rossi, Nucl. Phys. B (Proc. Suppl.) **50** (1996) 172; J. Huston et al., Phys. Rev. **D51** (1996) 6139; S. Frixione, M.L. Mangano, P. Nason, G. Rodolfi, Nucl. Phys. **B431** (1994) 453.; A. Breakstone et al., Z. Phys. **C52** (1991) 551; W.M. Geist at al, Phys. Rep. **197** (1990) 263; M. Della Negra et al., Nucl. Phys. **B127** (1977) 1

[19] T. Sjöstrand, Phys. Lett. **B157** (1985) 321

[20] M.A. Sanchis-Lozano and B. Cano, to appear in Nucl. Phys. B Proc. Suppl. (hep-ph/9611264)

[21] B. Cano and M.A. Sanchis-Lozano, IFIC/97-01 (hep-ph/9701210) to appear in Phys. Lett. B

[22] H. Plothow-Besch, 'PDFLIB: Nucleon, Pion and Photon Parton Density Functions and α_s', Users's Manual-Version 6.06, W5051 PDFLIB (1995) CERN-PPE

[23] J.P. Ma, UM-P-96/74 (hep-ph/9705445); P. Ko, SNUTP 96-084 (hep-ph/9608388)

[24] K. Sridhar, Mod. Phys. Lett. **A11** (1996) 1555